



Fabrication of carbon nanotube (CNTs)/Co₃O₄-Ni₃O₄/Al₂O₃ nanocomposite catalyst and its application for photocatalytic removal of celestine blue dye

Hussein Idrees Ismael,^a Ahmed F. Halbus,^{a*} Thamir A.H. Mohammad,^b

Sadiq J. Baqir,^b Zahraa H. Athab,^c Abbas J. Atiyah,^a Salih H. Kadhim,^a Emman J. Mohammad^a



^aDepartment of Chemistry, College of Science, University of Babylon, Hilla, IRAQ;

^bAlmustaqbal University College, Babylon, Hilla, IRAQ;

^cEnvironmental Research and Studies Center, University of Babylon, Hilla, IRAQ;

Abstract

In this work, we examined the photocatalytic activity of different composite ratios of doped co-oxide (Co₃O₄-Ni₃O₄/Al₂O₃) with carbon nanotubes (CNTs) toward Celestine blue dye (CBD). This work involves preparation of composite catalyst Co₃O₄-Ni₃O₄/Al₂O₃ doped with CNTs in different percent (2%, 4%, 6% and 8%) by using wet impregnation method. The prepared materials were characterized using Fourier transform infrared spectroscopy (FTIR), Atomic force microscope (AFM) and X-rays Diffraction technique (XRD). The photocatalytic activity of these materials were investigated by following photocatalytic removal of Celestine blue dye at $\lambda_{max} = 542\text{nm}$ and dye concentration equal to 100 ppm in different irradiation times. The obtained results showed that the best percent of doping the co-catalyst with carbon nanotubes was 6%, which gives a high photocatalytic dye removal equal to 99%.

Keywords: Co₃O₄-Ni₃O₄/Al₂O₃, carbon nanotube composite catalyst, photocatalytic activity, Celestine blue dye.

1. Introduction

Nanoscience has become one of the most important and interesting field in new science and technology due to many potential applications in various ways. Nanomaterials have new chemical, physical and mechanical properties better than their corresponding bulk materials, these new promising properties can enhance catalysis, photocatalytic activity, increasing strength, and other several interesting characteristics properties. Nanomaterials have different morphologies and structures consisting of clusters, sheets, quantum dots and nanotubes [1,2].

Among different types of nanomaterial's, carbon nanotubes can be considered to be very important

class due to it using in wide range of applications in nanotechnology sciences. These materials containing a series of carbon-carbon bonds as sp² hybridization in a hexagonal arrangement closely as honeycomb arrangement [3,4]. There are many types structures for CNTs, the first type is a single-walled CNTs (SWNTs), which is consisting of monolayer of graphene sheet that are rolled as a cylindrical shape with diameter around 1 nm. SWCNT classification to many types according the direction of the tube axis such as (a) semiconductor, metallic zigzag ($m=0$) (b) chiral ($n \geq 0$: $m \geq 0$) nanotubes and (c) metallic armchair ($n=m$) [5]. The second type is double wall CNTs (DWCNTs) which is result from rolled of two layers of graphene sheets into a

*Corresponding author e-mail: ahmed.halbus@uobabylon.edu.iq; (Ahmed F. Halbus).

Receive Date: 11 September 2021, Revise Date: 06 November 2021, Accept Date: 21 November 2021

DOI: 10.21608/EJCHEM.2021.95421.4480

©2019 National Information and Documentation Center (NIDOC)

cylindrical shape. The third type is similar to SWNTs structure which contains of 2-6 layers from graphene sheets which is called few walled carbon nanotubes (FWCNTs) [6]. The fourth type of CNTs is a multi-walled carbon nanotubes (MWCNTs) which is consisting of rolled many layers of graphene sheets [7].

According to the tube's diameter, warp direction and the helicity, CNTs behaves either as a semiconductor or metal [8]. CNTs have special

functionalization of MWCNTs improves its solubility in different solvents [15].

Carbon nanotubes supported on metal oxide nanoparticles have an effective properties that enable it to adsorb of many types of hazardous organic chemicals and heavy metal ions from water [16,17]. In this context it behaves as a catalyst. Nanocomposites materials have physical and chemical properties better than that of their components materials. This feature makes them show

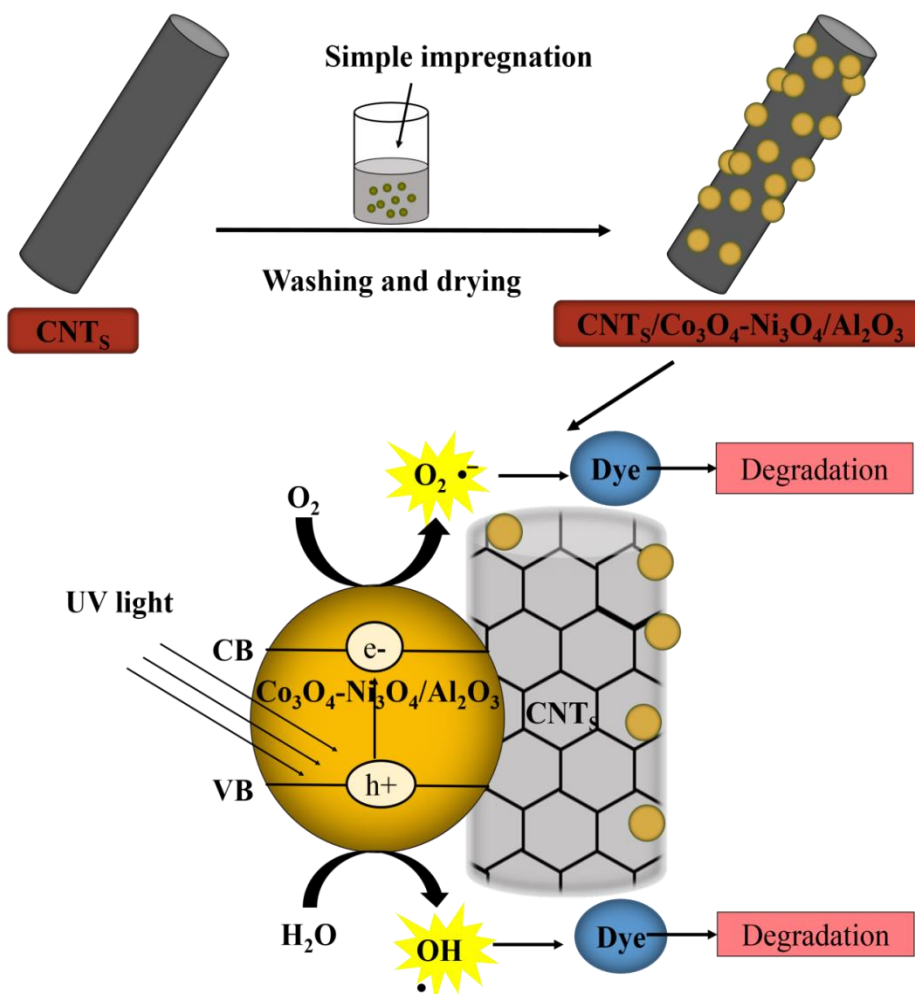


Fig. 1. Schematics showing the photocatalytic activity of the prepared nanocomposites materials with celestine blue dye.

optical, electrical, mechanical and thermal properties [9,10]. These properties make CNTs important and useful for high strength materials, sensors, fuel storage, nanoelectronics, energy storage, and biomedicine catalytic material for removal pollutant from waste water and air [11-14]. MWCNTs are difficult to dissolve in any solvent. But

higher catalytic activity in comparison with their corresponding single components[18].

Catalytic action occurs upon irradiation system which leads to generate (h⁺, e⁻) pairs in valence band and conduction band respectively of the co-oxide. Then conduction band electrons would transfer into CNTs surface which act as a sink for electrons that are generated at the co- oxides surface. Then it react

with adsorbed oxygen (O_{2ads}) to form O_2^- radical, from other hand, h^+ at the valence band contribute in formation of OH. These redox species can be contributed in redox reaction at the surface [19, 20]. These proposed action for mechanism is presented in Figure 1.

Alumina oxide considers as an important supported catalytic material, due to its high surface area, and it is an inert material so that it is widely used as a supported catalyst in heterogeneous catalysis. Its role in catalytic activity arises from its high surface area that prevent agglomeration of particles of catalyst and enhancement of catalytic activity for the catalytic process [21-23].

Cobalt oxide (Co₃O₄) is important photocatalyst and is used widely in many environmental

compounds that are found as pollutant in wastewater, nickel oxide is characterized by distorted structure, due to the presences of excess of oxygen in its crystal structure [26]. In terms of photocatalytic reactions that occur in presence of these oxides, the main drawback is the back electron transfer which occurs normally in neat photocatalyst, which leads to reduce the efficiency of the photocatalytic process. So that, combining these materials can reduce recombination rate with enhancement of the photocatalytic process [26-29].

The present study describes preparation of composite materials of co- Co₃O₄-Ni₃O₄/Al₂O₃ co-catalyst and functionalize carbon nanotubes in different ratios (2%, 4%, 6% and 8%). The novelty of the present work is presented by synthesis of the

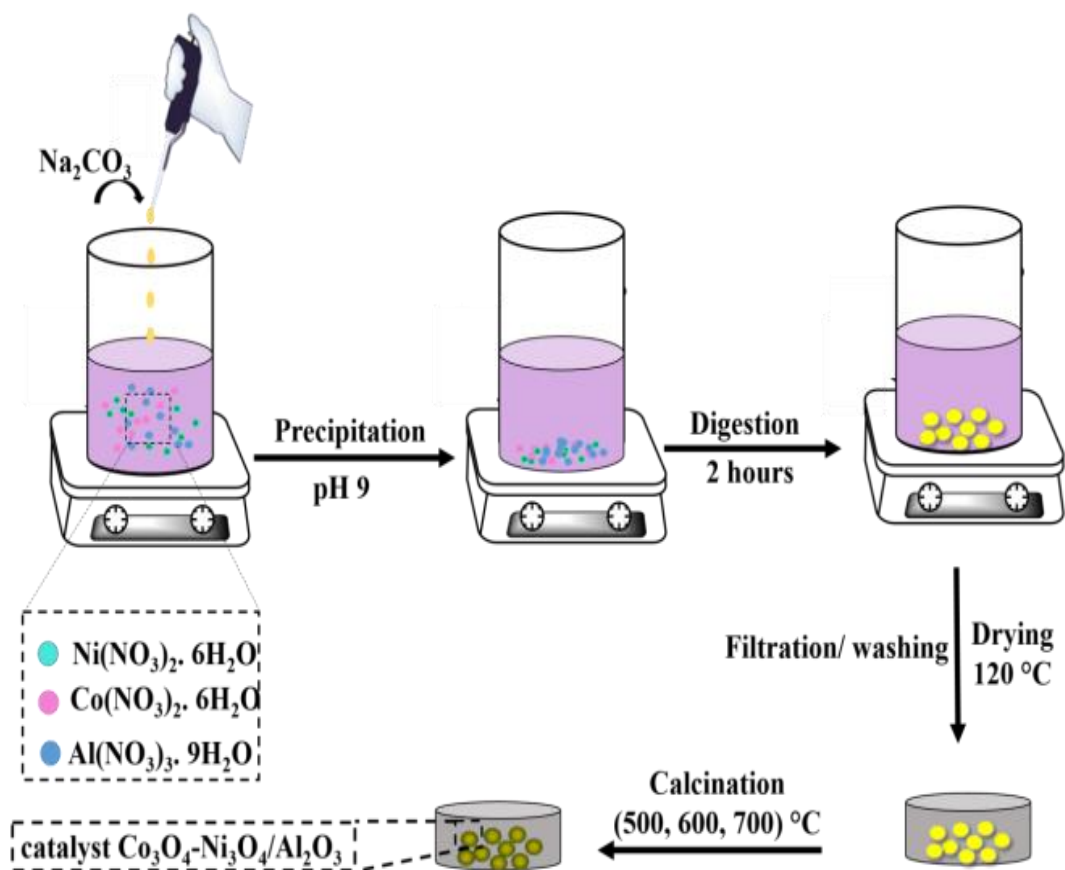


Fig. 2. Schematics showing the synthesis of CNTs/ Co₃O₄. Ni₃O₄/Al₂O₃ samples.

application such as such as colored glasses, electrochemical capacitors, in hydrogenation reactions, and removing pollutants from wastewaters. Besides that, it can be applied in oxidation of the volatile organic compounds [24,25].

On other hand, nickel oxide can be used in wide spectrum of applications such as removing

composite CNTs/Co₃O₄-Ni₃O₄/Al₂O₃ using eco-friendly materials with its application in Celestine blue dye removal by photocatalytic reactions. The reason for using CBD as a model in this work is due to its wide usage in many applications such as industrial, biological and environmental applications. So that large amounts of this dye are effluent to the

nearest environment and caused high level pollutions. The photocatalytic activity of the prepared nanocomposites materials would be investigated via monitoring removal of Celestine blue dye from its aqueous solutions (see Figure 1).

2. Experimental

Materials

All materials that were used in this work were in high purity, and provided from B.D.H. Nickel nitrate hexahydrate $\text{Ni}(\text{NO}_3)_2 \cdot 6\text{H}_2\text{O}$, Cobalt nitrate hexahydrate $\text{Co}(\text{NO}_3)_2 \cdot 6\text{H}_2\text{O}$ and Aluminum nitrate, $\text{Al}(\text{NO}_3)_3 \cdot 9\text{H}_2\text{O}$ were got from BDH Company with Purity 99.9%, 97.9% and 99.5% respectively. Sodium carbonate anhydrous Na_2CO_3 got from Gmbh with Purity 99.9%, HCl and NaOH were obtained from BDH Company. The used CNTs were MWCNTs provided from sigma Aldrich with a purity of 95%.

2.1. Methods

2.1.1. Synthesis of $\text{CNTs}/\text{Ni}_3\text{O}_4 \cdot \text{Co}_3\text{O}_4/\text{Al}_2\text{O}_3$ samples

The spinel catalyst $\text{Ni}_3\text{O}_4 \cdot \text{Co}_3\text{O}_4/\text{Al}_2\text{O}_3$ was prepared by co-precipitation method [30] in the ratio (30:30:40) for the components oxides respectively. Composites of co-catalyst and CNTs was prepared using different weights percent of CNTs (2%, 4%, 6% and 8%). These components were mixed homogeneously in wet using simple evaporation method, then dried in 120°C for 12 h. and calcinated at 600°C for 2 h. This is shown schematically in Figure 2.

The preparation was performed at basic media in order to achieve complete transformation of metal into metal carbonate which gives metal oxide after calcination at a proper temperature.

2.1.2. Photocatalytic activity of nanocomposites catalyst

Experiments of photocatalytic activity were conducted using a 30 mL photoreaction cell that was designed in the previous study as shown in Figure 3A. In each experiment, 0.05 g of nanocomposites catalyst was added to the solutions at different ratios (2%, 4%, 6% and 8%) to 30 mL of 100 ppm of Celestine blue dye.

The suspensions were stirred in darkness for 10 min using a magnetic stirrer (dark reaction) to ensure adsorption equilibrium has been occurred. Then irradiation of reaction mixture was initiated using mercury vapor lamp, then periodically 2 mL of reaction mixture were withdrawn at each 15 minute for a period of one hour.

Then suspension was centrifuged for 20 minute at a speed 5000 rpm. The absorbance of the supernatant liquid was measured at the maximum wavelength of

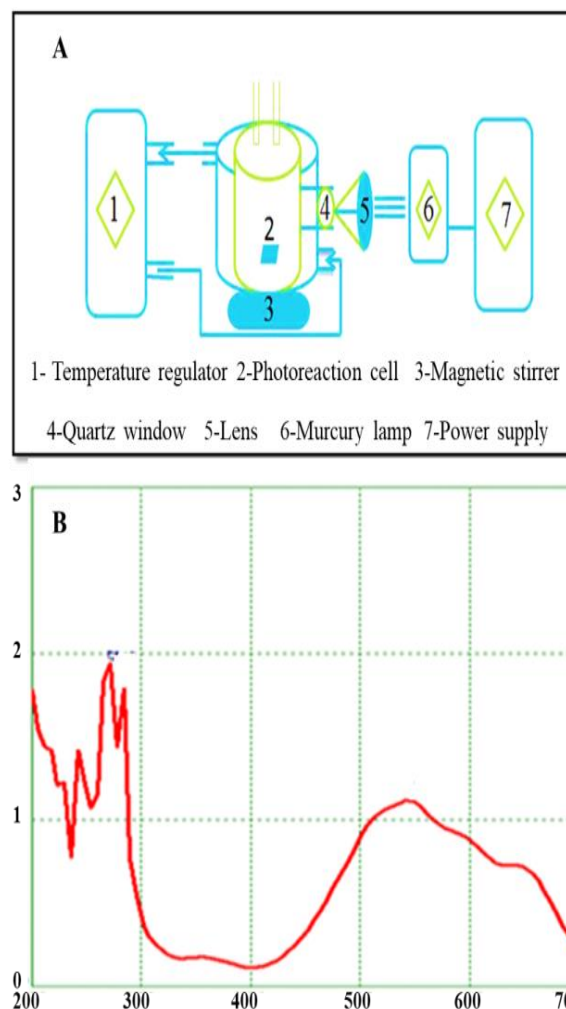


Fig. 3.(A) Homemade photoreaction system that was utilized in photocatalytic dye removal. (B) UV-visible spectra of Celestine blue dye, 100 ppm.

542 nm as shown in Figure 3B, Absorbance of Celestine blue dye without catalyst = 1.1126, which was measured with a UV-visible spectrophotometer type UV-Vis 1650PC Shimadzu, Japan.

3. Results and discussion

3.1. Characterization of CNTs/Ni₃O₄.Co₃O₄/Al₂O₃ catalyst

3.1.1. FTIR for the prepared composite

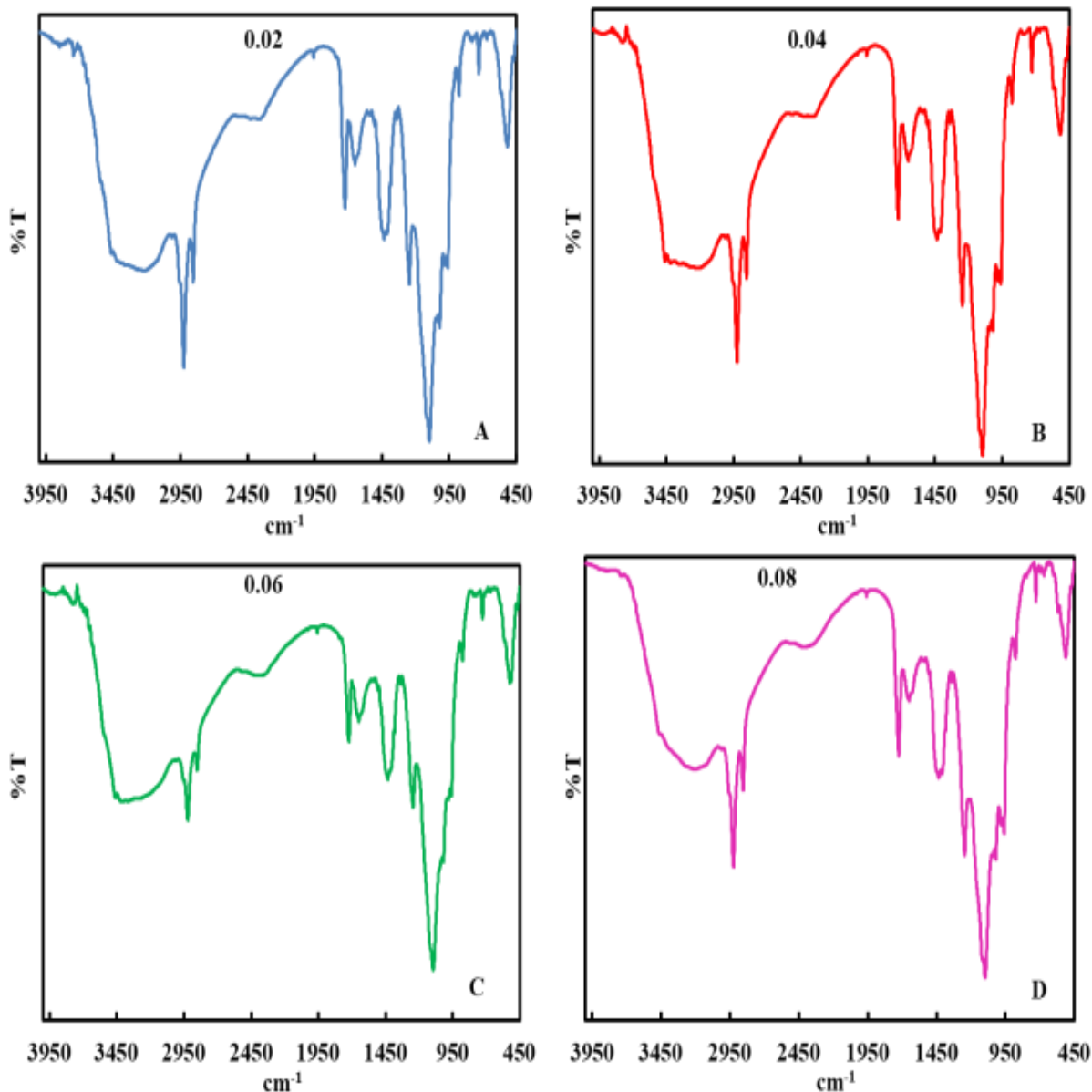


Fig. 4. FTIR spectra of different composite ratios of doped co-oxide (Co₃O₄-Ni₃O₄/Al₂O₃) with CNTs.

FTIR spectra of different composite ratios of doped co-oxide (Co₃O₄-Ni₃O₄/Al₂O₃) with CNTs are shown in Figure 4. In general, it can be seen that FTIR spectra for all doped samples are almost have similar peaks and show peaks that are related to both CNTs and co-oxide.

From these spectra, it can be seen that, the peaks around 420, 482 and 606 cm⁻¹ are related to the absorption of metal oxygen bond (M-O) bonds. These spectra show an absorption peak of nickel oxide around 420 and 482 cm⁻¹ and absorption peak at 606 and 520 cm⁻¹ for cobalt oxide [31,32]. The peak around 523-567 cm⁻¹ is due to Al₂O₃ [33]. The

peaks around 1650 and 3350-3470 cm⁻¹ can be assigned to the presence of surface hydroxyl group and due to adsorbed atmospheric water vapor. The broad peak in the range of 3100-3500 cm⁻¹ can be related to vibration modes of the surface hydroxyl group [34].

Also for these composites, the peak around 1633 cm^{-1} can be assigned to -C=C- of alkenes, and the peak around $1500\text{--}1400\text{ cm}^{-1}$ is assigned to the C–C stretching in the aromatic ring which may present with CNTs in the composite.

The sharp peak around 1741 cm^{-1} is assigned to C=O stretching vibrations of a carboxyl group at the surface of CNTs. The peak around 3394 cm^{-1} is assigned to the OH vibration [35].

Generally, FTIR spectra of the composites (CNTs/co-oxide/ Al_2O_3) show absorption peaks of each of co-oxide and CNTs in the composite in the four prepared samples.

The three main peaks correspond to metal-oxygen bonds in the range $432\text{--}619\text{ cm}^{-1}$, and the -OH bond around $1639\text{--}1681\text{ cm}^{-1}$, and OH bond vibration at 3383 cm^{-1} can be related to the intermolecular interaction at the surface of co-oxide with CNTs [36].

3.1.2. AFM of the composites

The surface morphology of synthesized CNTs/co-oxide/ Al_2O_3 was investigated using atomic force microscope (AFM), and the obtained results are presented in Figure 5. From these images it can be seen that all samples are shown high homogeneity and that probably arises from CNTs embedding with

the matrix of co-oxide for all doped ratios in this study (2% , 4%, 6% and 8%).

In this case, CNTs bundles easily bend and wrap around matrix of the co-oxide particles, this probably arises from strong interaction of functional groups of CNTs with that at present at co-oxide surface [37]. Besides that, this feature can be attributed to the high distribution of CNTs in the matrix of spinel and strong interactions between composites materials.

Also from these images, it can be seen that there was a relative reduction in grain size with increasing ratio of the doped CNTs from 2% up to 6%. At higher ratio 8% it can be seen that there was an increase in grain size.

This probably due to relatively high doped ratio under these circumstances. It is clear that reduction in grain size and particle size leads to increase of the surface area of the used catalytic materials, which results in increasing of catalytic activity of the interested material.

These observations are consistent with the obtained results in this study as the composite CNTs/co-oxide/ Al_2O_3 in a ratio of 6% showed higher catalytic activity in terms of photocatalytic removal of CBD under these reaction conditions in comparison with other composites [38].

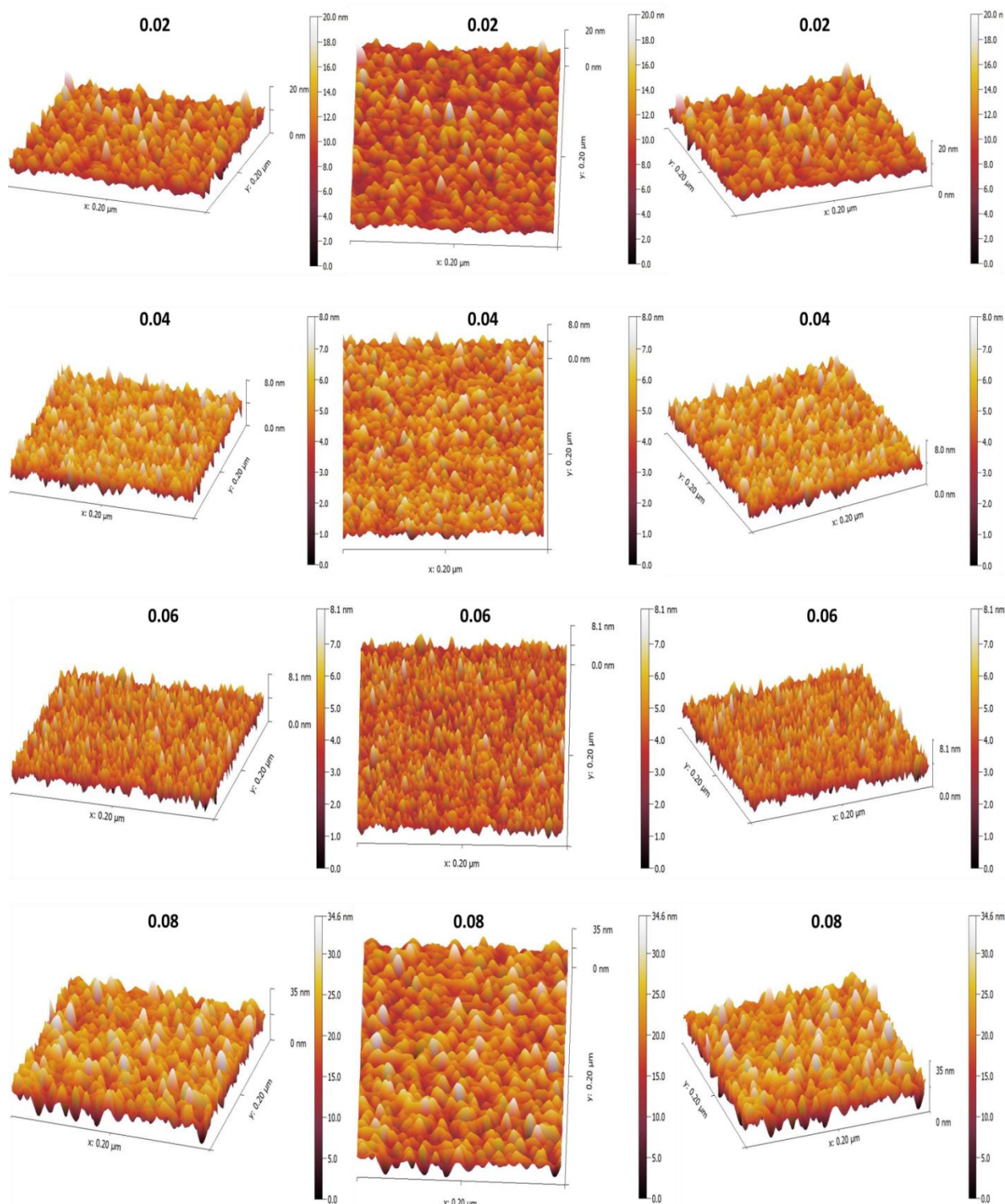


Fig. 5. AFM of different composite ratios of doped co-oxide (Co₃O₄-Ni₃O₄/Al₂O₃) with CNTs.

Crystal structure of the prepared materials was investigated using Phillips X-rays diffraction in the range of 2θ 10–80 degrees. Powder X-rays diffraction

patterns (PXRD) of the prepared nanocomposites at weight ratios 6% of CNTs and catalyst without CNTs are shown in Figure 6. PXRD patterns of the composite are extremely similar to that of spinel

catalysts with appear peaks at $2\theta=26.5, 33.9$ and 44.3 for CNTs. From these patterns, it can be seen that there were some deviations in the d-spaces and peaks positions when comparing with the standard values (JPCDS). This deviation is acquired by influencing and overlapping between CNTs and oxides [39,40].

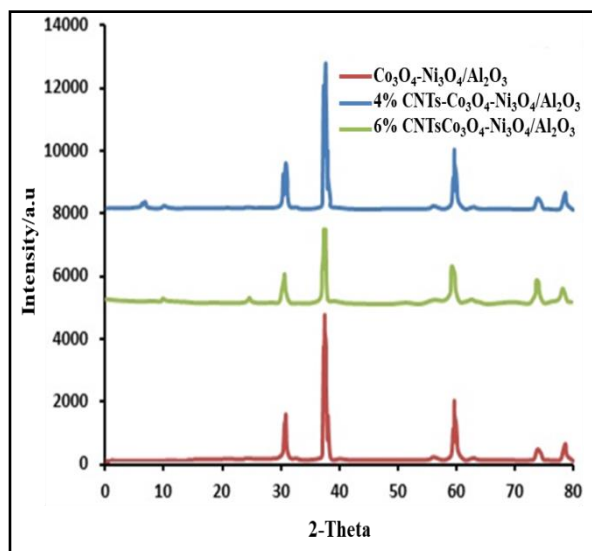


Fig. 6. XRD patterns for $\text{Co}_3\text{O}_4\text{-Ni}_3\text{O}_4/\text{Al}_2\text{O}_3$ and $\text{CNTs}/\text{Co}_3\text{O}_4\text{-Ni}_3\text{O}_4/\text{Al}_2\text{O}_3$.

3.1.3. Photocatalytic activity of the prepared nanocomposites catalyst

Several experiments were performed to investigate the best ratios of the nanocomposites catalyst that was calcinated at 600°C and it was found that the best ratio was 6%. This catalyst was chosen to be the best one due to have better physical properties and good catalytic performance in redox reactions and removing environmental pollution into the aqueous solution [41-46], it was also found that the CNT good adsorbed material due to have higher surface area. Figure 7 and Table 1 show the best ratio of prepared nanocomposites. The efficiency of dye removal was determined using the equation [47-51]:

$$\text{Remaining percentage} = A_t / A_0$$

Where the A_0 , A_t , is the initial and the final absorption of dye.

Table 1. Absorbance of Celestine blue dye over different percent of $\text{CNTs}/\text{Co}_3\text{O}_4\text{-Ni}_3\text{O}_4/\text{Al}_2\text{O}_3$ and $\text{Co}_3\text{O}_4\text{-Ni}_3\text{O}_4/\text{Al}_2\text{O}_3$ at different time.

Time/min	2% CNTs	4% CNTs	6% CNTs	8% CNTs	$\text{Co}_3\text{O}_4\text{-Ni}_3\text{O}_4/\text{Al}_2\text{O}_3$
15	0.032	0.045	0.0261	0.042	0.055
30	0.025	0.039	0.0232	0.038	0.046
45	0.019	0.036	0.0188	0.034	0.042
60	0.018	0.031	0.0123	0.029	0.034

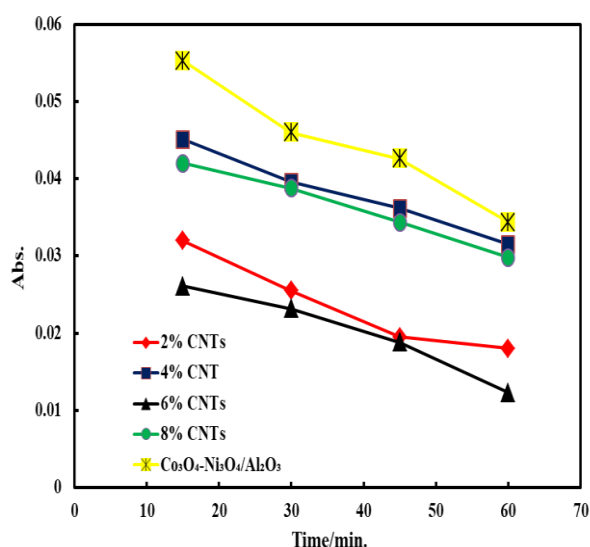


Fig. 7. Absorbance of Celestine blue dye over different percent of $\text{CNTs}/\text{Co}_3\text{O}_4\text{-Ni}_3\text{O}_4/\text{Al}_2\text{O}_3$ and $\text{Co}_3\text{O}_4\text{-Ni}_3\text{O}_4/\text{Al}_2\text{O}_3$.

The best ratio of the prepared CNTs composite catalyst was 6% CNTs which gives high efficiency for removal of dye approach to 99% as shown in Figure 8, this may be due to increasing of their surface area and porosity and increasing of active pore sites and give the best distribution of these active sites [52].

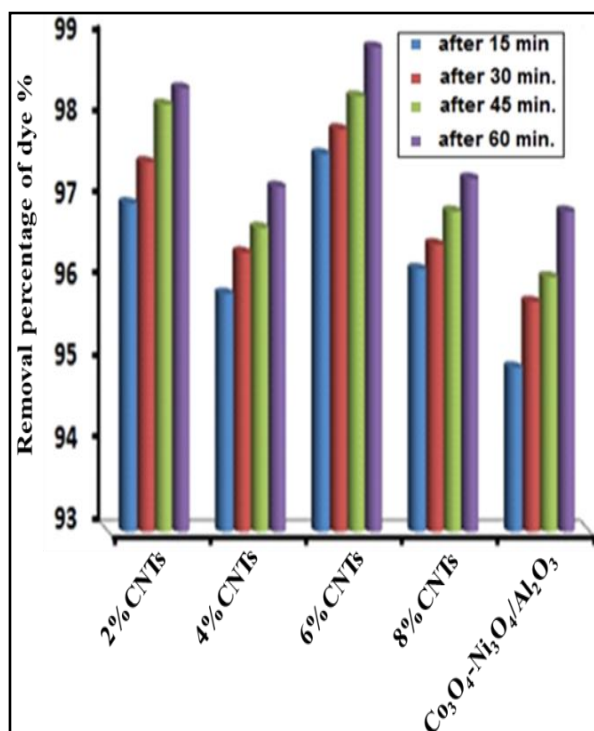


Fig. 8. Removal percentage of Celestine blue dye over different ratios of CNTs Composite and Co₃O₄-Ni₃O₄/Al₂O₃.

4. Conclusions

Here, we described the synthesis and characterisation of various composite ratios of doped co-oxide (Co₃O₄-Ni₃O₄/Al₂O₃) with CNTs, including Fourier transform infrared spectroscopy, atomic force microscope and X-ray diffraction. The results from FTIR spectra of different composite ratios of doped co-oxide Co₃O₄-Ni₃O₄/Al₂O₃ with CNTs showed that the absorption peaks of each of co-oxide and CNTs in the composite in the four prepared samples. The three main peaks correspond to metal-oxygen bonds in the range 432–619 cm⁻¹, and the -OH bond around 1639–1681 cm⁻¹, and OH bond vibration at 3383 cm⁻¹ can be related to the intermolecular interaction at the surface of co-oxide with CNTs. The results from AFM analysis showed that all samples are shown high homogeneity and that probably arises from CNTs embedding with the matrix of co-oxide for all

doped ratios in this study (2%, 4%, 6% and 8%). Also from AFM images, it was discovered that there was a relative reduction in grain size with increasing ratio of the doped CNTs from 2% up to 6%. At higher ratio 8% it can be seen that there was an increase in grain size. This probably due to relatively high doped ratio under these circumstances. From the obtained results in this work, we also show that the best ratio of the prepared nanocomposites catalyst was 6% CNTs/ Co₃O₄-Ni₃O₄/Al₂O₃, which showed high photocatalytic activity for degradation of Celestine blue dye in concentration of 100 ppm for 60 min in room temperature.

5. Conflicts of interest

“There are no conflicts to declare”.

6. Acknowledgments

The authors would like to thank University of Babylon, College of Science in Iraq for funding this work as a part of annual research plan for academic staff.

7. References

- [1] T. Masciangioli, W. X. Zhang, Peer reviewed: environmental technologies at the nanoscale, environmental science and technology, 2003, **37**, 102-108.
- [2] Z. H. Athab, A. F. Halbus, G. M. Greenway, A Simple method for the synthesis of high surface area mesoporous carbon monolith via soft template technique, Egyptian Journal of Chemistry, 2021, **64(10)**, 5793 – 5801.
- [3] C. Darnault, K. Rockne, A. Stevens, G. A. Mansoori, N. Sturchio, Fate of environmental pollutants, Water Environment Res, 2005, **77**, 2576.
- [4] G. A. Mansoori, T. R. Bastami, A. Z. Ahmadpour, Eshaghi. environmental application of nanotechnology, Ann. Rev. Nano Res, 2008, **2**, 1.
- [5] S. Iijima, T. Ichihashi, D. S. Bethune, C. H. Kiang, M. S. DeVries, G. Gorman, R. Savoy, R. Beyers, Synthesis of multiwalled carbon nanotubes from carbon black, Nature, 1993, **363**, 605.

- [6] M. Okada, S. Igimi, T. Inoue, X. Cheng, R. Xiang, S. Chiashi, Y. Inoue, Y. Wang, S. Maruyama, Dry drawability of few-walled carbon nanotubes grown by alcohol chemical vapor deposition, *The Journal of Physical Chemistry C*, 2020, **124**(31), 17331-17339.
- [7] H. Kroto, J. Heath, S. Brin, R. Curl, R. Smally, C₆₀: buckminsterfullerene, *Nature*, 1985, **318**, 162-163.
- [8] O. Yuy, P. Jing-Cui, W. Hui, P. Zhi-Hua, The rehybridization of electronic orbitals in carbon nanotubes, *Chinese Phys. B*, 2008, **17**, 3123-3129.
- [9] K. Zare, F. Najafi, H. Sadegh, Studies of ab initio and Monte Carlo simulation on interaction of fluorouracil anticancer drug with carbon nanotube, *J Nanostruc Chem*, 2013, **3**(1), 1-8.
- [10] E.T. Thostenson, Z. F. Ren, T.W. Chou, Advances in the science and technology of carbon nanotubes and their composites: a review, *Compos Sci Technol*, 2001, **61**(13), 1899-1912.
- [11] L-M. Peng, Z. Zhang, S. Wang, Carbon nanotube electronics: recent advances, *Mater Today*, 2014, **17** (9), 433-442.
- [12] A. Szabó, C. Perri, A. Csató, G. Giordano, D. Vuono, J.B. Nagy, Synthesis methods of carbon nanotubes and related materials, *Materials*, 2010, **3**(5), 3092-3140.
- [13] D. Antiohos, M. Romano, J. Chen, J. M. Razal, Carbon nanotubes for energy applications, 2013, DOI: 10.5772/51784.
- [14] G. Wang, L. Zhang, J. Zhang, A review of electrode materials for electrochemical supercapacitors, *Chem Soc Rev*, 2012, **41**(2), 797-828.
- [15] A. Star, J. F. Stoddart, D. Steuerman, M. Diehl, A. Boukai, E. W. Wong, X. Yang, S. W. Chung, H. Choi, J.R. Heath, Preparation and properties of polymer-wrapped single-walled carbon nanotubes. *Angewandte Chemie-International Edition*, 2001, **40**(9), 1721-1725.
- [16] A. Gadhave, J. Waghmare, Removal of heavy metal ions from wastewater by carbon nanotubes (CNTs), *International Journal of Chemical Sciences and Applications*, 2014, **5**(2), 56-67.
- [17] V. K. Gupta, S. Agarwal, T. A. Saleh, Synthesis and characterization of alumina coated carbon nanotubes and their application for lead removal, *Journal of Hazardous Materials*, 2011, **185**(1), 17-23.
- [18] A. F. Halbus, T. S. Horozov, V. N. Paunov, Self-grafting copper oxide nanoparticles show a strong enhancement of their anti-algal and anti-yeast action, *Nanoscale Advances*, 2019, **1**(6), 2323-36.
- [19] A. Ajmal, I. Majeed, R. N. Malik, H. Idriss, M. A. Nadeem, Principles and mechanisms of photocatalytic dye degradation on TiO₂ based photocatalysts: a comparative overview, *Rsc Advances*, 2014, **4**(70), 37003-37026.
- [20] M. A. Rauf, S. S. Ashraf, Fundamental principles and application of heterogeneous photocatalytic degradation of dyes in solution, *Chemical engineering journal*, 2009, **151**(1-3), 10-18.
- [21] C. H. Bartholomew, R. J. Farrauto, Fundamentals of industrial catalytic processes, John Wiley and Sons, 2011.
- [22] A. Z. Ziva, Y. K. Suryana, Y. S. Kurniadianti, A. B. D. Nandiyanto, T. Kurniawan, Recent Progress on the Production of Aluminum Oxide (Al₂O₃) Nanoparticles: A Review. *Mechanical Engineering for Society and Industry*, 2021, **1**(2), 54-77.
- [23] Y. O. Leonova, M. A. Sevostyanov, D. O. Mezentsev, D. R. Khayrutdinova, A. S. Lysenkov, Effect of the synthesis temperature on the phase composition of Al₂O₃. In *Journal of Physics: Conference Series*, 2021, 1942(1), 012052.
- [24] A. D. Jagdale, V. S. Kumbhar, R. N. Bulakhe, C. D. Lokhande, Influence of electro deposition modes on the supercapacitive performance of Co₃O₄ electrodes, *Energy*, 2014, **64**, 234-241.
- [25] R. Kumar, A. Soam, V. Sahajwalla, Carbon coated cobalt oxide (CC-CO₃O₄) as electrode material for supercapacitor applications, *Materials Advances*, 2021, **2**(9), 2918-2923.
- [26] S. J. Hong, H. J. Mun, B. J. Kim, Y. S. Kim, Characterization of nickel oxide nanoparticles synthesized under low temperature, *Micromachines*, 2021, **12**(10), 1168.
- [27] M. Pawar, S. TopcuSendoğdular, P. Gouma, A brief overview of TiO₂ photocatalyst for organic dye remediation: case study of reaction mechanisms involved in Ce-TiO₂ photocatalysts system, *Journal of Nanomaterials*, 2018, **2018**, 1-3.
- [28] F. M. Khandan, D. Afzali, G. Sargazi, M. Gordan, Novel uranyl-curcumin-MOF photocatalysts with highly performance photocatalytic activity toward the degradation of

- phenol red from aqueous solution: Effective synthesis route, design and a controllable systematic study, *Journal of Materials Science: Materials in Electronics*, 2018, **29(21)**, 18600-18613.
- [29] G. Sargazi, A. K. Ebrahimi, D. Afzali, A. Badoei-dalfard, S. Malekabadi, Z. Karami, Fabrication of PVA/ZnO fibrous composite polymer as a novel sorbent for arsenic removal: design and a systematic study, *Polymer Bulletin*, 2019, **76(11)**, 5661-5682.
- [30] E. J. Mohammad, A. J. Lafta, S. H. Kadhim, Photocatalytic removal of reactive yellow 145 dye from simulated textile wastewaters over supported (Co, Ni)₃O₄/Al₂O₃ co-catalyst, *Polish Journal of Chemical Technology*, 2016, **18(3)**, 1-9.
- [31] I. P. Okoye, C. Obi, Thermodynamic and kinetic evaluations of some heavy metal ions on aluminum-pillared and unpillared bentonite clays, *International Archive of Applied Sciences and Technology*, 2012, **3(2)**, 58-67.
- [32] M. Julkarnain, J. Hossain, K.S. Sharif, K.A. Khan, Optical properties of thermally evaporated Cr₂O₃ thin films, *Canadian Journal on Chemical Engineering & Technology*, 2012, **3(4)**, 81-85.
- [33] S. P. Ghosh, Synthesis and characterization of zinc oxide nanoparticles by sol-gel process, 2012.
- [34] H. Cao, X. Qiu, Y. Liang, M. Zhao, Q. Zhu, Sol-gel synthesis and photoluminescence of p-type semiconductor Cr₂O₃ nanowires, *Applied physics letters*, 2006, **88(24)**, 241112.
- [35] N.I. Kovtyukhova, T.E. Mallouk, L. Pan, E.C. Dickey, Individual single-walled nanotubes and hydrogels made by oxidative exfoliation of carbon nanotube ropes, *Journal of the American Chemical Society*, 2003, **125(32)**, 9761-9769.
- [36] A. Yildirim, T. Seckin, In situ preparation of polyether amine functionalized MWCNT nanofiller as reinforcing agents, *Advances in Mater. Sci. Eng.*, ID 356920, 1(2014).
- [37] S.K. Kim, H.S. Park, Multiwalled carbon nanotubes coated with a thin carbon layer for use as composite electrodes in supercapacitors, *RSC Adv.*, 2014, **4(88)**, 47827-47832.
- [38] Y. Yao, G. Li, S. Ciston, R.M. Lueptow, K.A. Gray, Photoreactive TiO₂/carbon nanotube composites: synthesis and reactivity, *Environmental science & technology*, 2008, **42(13)**, 4952-4957.
- [39] E. J. Mohammad, M. M. Kareem, A. J. Atiyah, Synthesis of carbon nanotubes from graphite and investigation of the catalytic activity of MWCNTs/Cr₂O₃-NiO with the removal of bismarck brown G dye from its aqueous solution, *Ukr. J. Phys*, 2019, **64(4)**, 2071-0186.
- [40] C. Kao, R. Young, A Raman spectroscopic investigation of heating effects and the deformation behavior of epoxy/SWNT composites, *Composites Sci. Tech*, 2004, **64**, 2291.
- [41] F. H. Hussein, A. F. Halbus, A. J. Lafta, Z. H. Athab, Preparation and characterization of activated carbon from iraqi khestawy date palm, *J Chem*, 2015, 1-8.
- [42] A. N. Al-Sharify, Z. H. Athab, A. F. Halbus, Adsorption of Reactive Red 2 dye onto activated carbon prepared from hazelnut shells, *Iraqi Natl J Chem*, 2013, **51**, 273-287.
- [43] F. H. Hussein, A. F. Halbus, F. H. Abdalrazak, Z. H. Athab, Adsorption of cobalamin onto synthesized carbon nanotubes (CNT), 2013, **2(3)**, 589-604.
- [44] A. F. Halbus, J. M. Salman, A. J. Lafta et al, Equilibrium, isotherms and thermodynamic studies of Congo red adsorption onto ceratophyllum demersum, *Indian J Chem Technol*, 2017, **24(1)**, 82-87.
- [45] H. A. Zahraa, Production and characterization of activated carbon from Iraqi palm fiber, *Asian J Chem*, 2015, **27(10)**, 3658-3662.
- [46] A. F. Halbus, Z. H. Athab, F. H. Hussein, Adsorption of disperse blue dye on Iraqi date palm seeds activated carbon, *Int J Chem Sci*, 2013, **11(3)**, 1219-1233.
- [47] A. F. Halbus, A. J. Lafta, Z. H. Athab, F. H. Hussein, Adsorption of reactive yellow dye 145 from wastewater onto Iraqi zahdy and khestawy date palm seeds activated carbons, *Asian J Chem*, 2014, **26**, S167-S172.
- [48] A. J. Lafta, A. F. Halbus, F. S. Daabool, Z. S. Burhan, H. A. Fenoan, F. H. Hussein, Adsorption of reactive yellow-145 dye on activated carbons, *Int J Chem*, 2014, **3**, 179-183.
- [49] A. J. Lafta, A. F. Halbus, S. J. Baqir, F. H. Hussein, Removal of reactive yellow 145 dye from simulated industrial wastewaters on Iraqi khestawy date palm seeds based activated carbons, *Res J Pharm Biol Chem Sci*, 2015, **6(6)**, 1115-1123.

-
- [50]A. J. Lafta, A. F. Halbus, Z. H. Athab et al, Effects of activators on adsorption ability of reactive yellow-145 dye on activated carbon from Iraqi zahdi date palm seeds, *Asian J Chem*, 2014, **26**, S119-S123.
- [51]A. F. Halbus, Z. H. Athab, F. H. Hussein, Review on preparation and characterization of activated carbon from low cost waste materials, *Egyptian Journal of Chemistry*, 2021.
- [52]S.H. Kadhim, T.H. Mgheer, H.I. Ismael, Kh.J. Kadem, A.S. Abbas, A.J. Atiyah, E. J. Mohammad, Synthesis, characterization and catalytic activity of NiO-CoO-MgO Nano-Composite Catalyst, *Indones. J. Chem.*, 2019, **19(3)**, 675-683.